

Synthesis and electrochemical properties of numerous classes of vanadates

S. Denis ^a, E. Baudrin ^a, F. Orsini ^a, G. Ouvrard ^{b,*}, M. Touboul ^a, J.-M. Tarascon ^a

^a Laboratoire de Réactivité et de Chimie des Solides, UPRES A 6007 CNRS, 33 Rue Saint-Leu, 80039 Amiens Cedex, France

^b Institut des Matériaux de Nantes, 2 rue de la Houssinière, BP 32229, 44322 Nantes Cedex 3, France

Abstract

Several classes of vanadates can be synthesized by a ‘chimie douce’ method, which consists of a precipitation reaction occurring at a well-defined pH. An electrochemical investigation has shown that these compounds, depending on their amorphous/crystallized nature, can react with large amounts of Li, leading to reversible capacities as large as 900 mA h/g. Both electrochemical and in situ X-ray diffraction studies suggest that a mechanism of Li uptake/removal, different from the usual Li insertion/deinsertion process, is occurring in these vanadates. © 1999 Elsevier Science S.A. All rights reserved.

Keywords: Vanadates; Chimie douce; Anode material; Li-ion battery

1. Introduction

Within the field of energy storage, vanadates have recently generated a new interest as these compounds were shown to be potential candidates for negative electrode material in lithium-ion battery. Indeed, it was previously reported that such material-based electrodes display a large Li acceptance/removal at low voltage. For instance, crystallized LiNiVO_4 , synthesized by the classical high temperature route can react with 7 lithium ions per formula unit when discharged to voltages lower than 0.2 V [1], leading to 800–900 mA h/g specific capacities, about twice as large as the actually used graphite electrodes. However, upon the first electrochemical discharge, it was noted that these materials tend to become amorphous; therefore, a slow cycling rate is needed to properly achieve their formation step.

As an attempt to alleviate this issue, a ‘chimie douce’ method was employed in order to directly prepare these vanadates in an amorphous state. Herein, we report on the ability to prepare several classes of vanadates through the use of a low temperature process from a mixed solution of NH_4VO_3 and nitrate salts. Depending on the nature and the charge of the counter cation, amorphous or crystallized vanadates can be obtained. An electrochemical investigation has confirmed the great interest in amorphous vana-

dates as negative electrode material in Li-ion rechargeable batteries [2].

In order to explain the great acceptance of lithium ions within these materials, a Li reaction mechanism different from the classical insertion/deinsertion process will be proposed, based on in situ XRD and XANES measurements.

2. Experimental

2.1. Characterization

Thermal analyses were performed using a Setaram (TG-DTA92) type equipment on sample weights of about 20 mg and with a heating rate of 10°C/min. X-ray powder diffraction patterns were recorded by means of a Philips diffractometer (PW1710) using the Cu K_{α} radiation ($\lambda = 1.5418 \text{ \AA}$), and of a Siemens (D5000) diffractometer (using the Cu $K_{\alpha 1}$ radiation $\lambda = 1.5406 \text{ \AA}$) with a homemade electrochemical cell for in situ measurements. The ratio Metal/V was checked for all the synthesized compounds with an EDS analyzer (Link Oxford).

2.2. Electrochemical measurements

Swagelok™ test cells were built using vanadate as the active positive electrode material, and Li metal as the

* Corresponding author

active negative electrode material, both separated by a glass fibre separator soaked in a 1 M LiPF_6 in EC:DMC (2:1 in weight ratio) electrolyte solution. The plastic positive electrode was elaborated using the Bellcore's PLiON™ technology, which was described elsewhere [2]. Electrochemical measurements were carried out by means of a 'Mac-Pile' system (Biologic, Claix, France) operating in a galvanostatic mode.

3. Synthesis method

The starting materials are ammonium metavanadate (NH_4VO_3) and the nitrate of the desired element (called counter cation). The synthesis method consists in mixing a NH_4VO_3 solution with a nitrate solution in stoichiometric amounts and then controlling the pH. We will show later that the pH is strongly dependent on the counter cation charge. The pH value of the mixture is firstly decreased to a value denoted hereafter 'lower pH' using a nitric acid solution, and then raised by means of an ammoniacal solution to a pH value for which pure phases are obtained. The precipitate is then recovered by centrifugation, washed with water and acetone, and dried overnight at 50°C in an oven.

3.1. Results

For divalent element based vanadates (Co or Ni), several types of hydrated vanadates can be prepared as a function of the pH of the media (Table 1). Note that $(\text{NH}_4)_2\text{M}_2\text{V}_{10}\text{O}_{28} \cdot 16\text{H}_2\text{O}$ and $\text{M}(\text{VO}_3)_2 \cdot 4\text{H}_2\text{O}$ are crystallized while $\text{M}_3(\text{VO}_4)_2 \cdot n\text{H}_2\text{O}$ is amorphous. $\text{M}_2\text{V}_2\text{O}_7 \cdot n\text{H}_2\text{O}$ is amorphous or crystallized depending on the n value.

Concerning mixed monovalent–divalent element based vanadates, a new amorphous hydrated compound $\text{LiNiVO}_4 \cdot 2.6\text{H}_2\text{O}$, precursor of the well-known spinel LiNiVO_4 , was recently synthesized [4]. This material was only obtained by operating at pH 8.5 in a large excess of lithium. The initial molar ratio Li:Ni:V has to be equal at least to 15:1:1.

Finally, for the synthesis of trivalent element vanadates (In, Cr, Fe and Al), a precipitation instantaneously occurs upon mixing the starting materials solutions. The pH is then lowered to 1, and then adjusted to 4 in order to obtain

Table 1
pH values for the synthesis of divalent element vanadates ($\text{M} = \text{Co}, \text{Ni}$) [3]

Compound	Lower pH value	pH of obtainment
$(\text{NH}_4)_2\text{M}_2\text{V}_{10}\text{O}_{28} \cdot 16\text{H}_2\text{O}$	2.5	5.3
$\text{M}(\text{VO}_3)_2 \cdot 4\text{H}_2\text{O}$	3	6
$\text{M}_2\text{V}_2\text{O}_7 \cdot n\text{H}_2\text{O}$	3	6.5
$\text{M}_3(\text{VO}_4)_2 \cdot n\text{H}_2\text{O}$	3	8

Table 2
pH values for the synthesis of several orthovanadates [3]

Compound	pH of obtainment
$\text{RVO}_4 \cdot n\text{H}_2\text{O}$ ($\text{R} = \text{In}, \text{Cr}, \text{Fe}, \text{Al}$)	4
$\text{Co}_3(\text{VO}_4)_2 \cdot n\text{H}_2\text{O}$	8
$\text{LiNiVO}_4 \cdot 2.6\text{H}_2\text{O}$	8.5
Li_3VO_4	~ 12

phases of good purity. All the synthesized compounds have the general formula $\text{RVO}_4 \cdot n\text{H}_2\text{O}$ (R being the trivalent element), and are amorphous as determined by X-ray diffraction measurements.

3.2. Discussion

We now review the different classes of vanadates and the pH conditions during the synthesis in order to determine general trends, and rationalize the synthesis method. Two parameters have to be considered for the oxide formation in solution: (i) the role of the vanadate anion type and (ii) the role of the counter cation.

(i) For a fixed counter cation (for example Co^{2+}), several classes of vanadates can be obtained depending on the pH conditions. According to the results reported in Table 1, the lower the obtainment pH is, the more condensed the vanadate polyanion species are (i.e., they are formed by an increasing number of molecular units). This evolution is in good agreement with the distribution diagram of isopolyvanadates [5] in solution as a function of the pH.

(ii) For a fixed anion (for example VO_4^{3-}), the pH of obtainment of the vanadate depends on the charge of the counter cation (Table 2).

To explain this evolution, we can refer to the cation charge–pH diagram [6]. In an aqueous solution, the first coordination sphere of a cation may contain aquo, hydroxo and/or oxo species. In our case, the cation is initially in an aquo form. In order to condense, it must enter the hydroxo zone, emphasizing the importance of the pH. According to

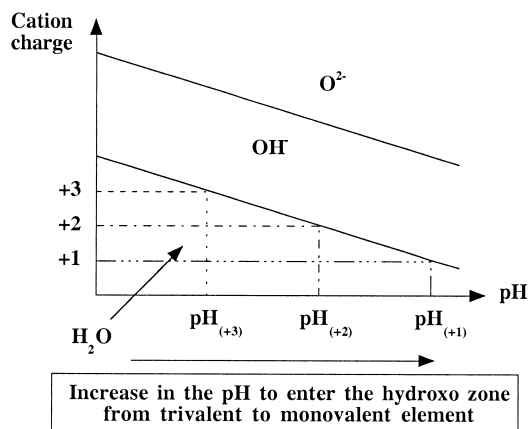


Fig. 1. Cation charge–pH diagram showing the obtainment pH evolution for one vanadate type.

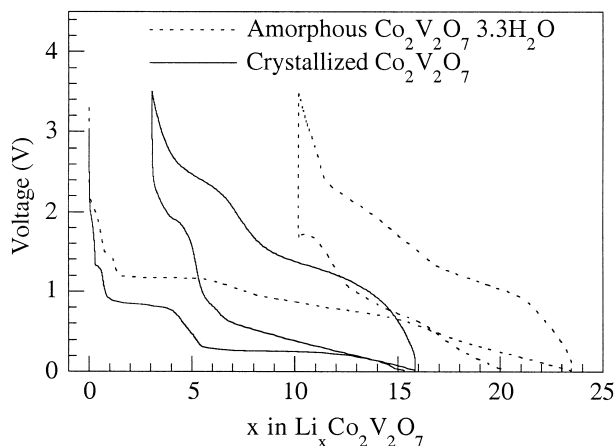


Fig. 2. Voltage vs. composition profile curves of $\text{Co}_2\text{V}_2\text{O}_7 \cdot 3.3\text{H}_2\text{O}$ and $\text{Co}_2\text{V}_2\text{O}_7/\text{Li}$ batteries.

this charge–pH diagram and our results, hydroxo groups form at lower pH with increasing the charge of the counter cation (Fig. 1).

4. Electrochemical properties

4.1. $\text{Co}_2\text{V}_2\text{O}_7 \cdot 3.3\text{H}_2\text{O}$ and $\text{Co}_2\text{V}_2\text{O}_7$

Fig. 2 compares the voltage vs. lithium content curves for crystallized $\text{Co}_2\text{V}_2\text{O}_7 \cdot 3.3\text{H}_2\text{O}$ and $\text{Co}_2\text{V}_2\text{O}_7$ (prepared by annealing the former at 500°C). Data are given for the first cycle recorded at a rate of 1 Li in 2 h, and for voltages ranging from 0.02 V to 3.5 V.

Upon the first electrochemical discharge, crystallized $\text{Co}_2\text{V}_2\text{O}_7 \cdot 3.3\text{H}_2\text{O}$ can react with about 23 lithium ions per formula unit. However, only 13 lithium ions can be removed during the following charge of the battery. Comparatively, crystallized $\text{Co}_2\text{V}_2\text{O}_7$ reversibly reacts with 12 lithium ions, resulting in capacities as large as 1000 mA h/g, that is twice and a half as great as than the capacity

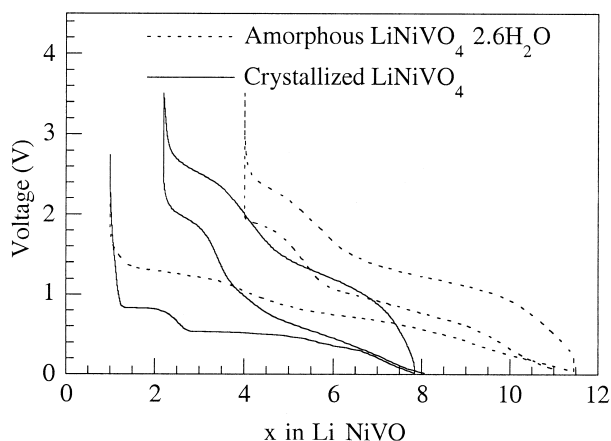


Fig. 3. Voltage vs. composition profile curves of $\text{LiNiVO}_4 \cdot 2.6\text{H}_2\text{O}$ and $\text{LiNiVO}_4/\text{Li}$ batteries [4].

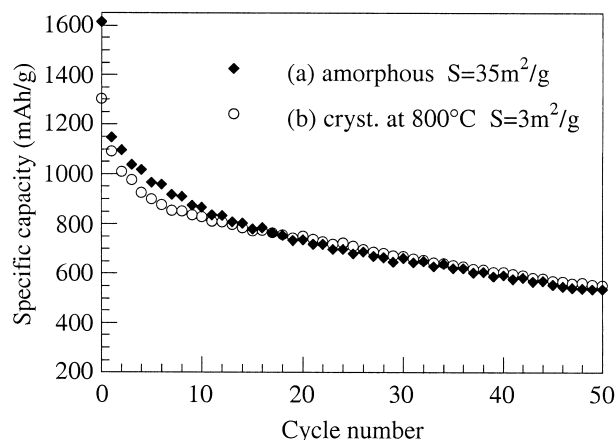


Fig. 4. Cycling behavior of $\text{LiNiVO}_4 \cdot 2.6\text{H}_2\text{O}$ and $\text{LiNiVO}_4/\text{Li}$ batteries [4].

of conventional graphite electrode. Note also that the irreversible capacity loss between the first discharge and charge is about three times lower for this anhydrous crystallized vanadate compared with $\text{Co}_2\text{V}_2\text{O}_7 \cdot 3.3\text{H}_2\text{O}$ (3 vs. 10 lithium ions). The difference in the irreversible capacity loss may be induced by the presence of water molecules.

4.2. LiNiVO_4

As previously reported [4], both amorphous $\text{LiNiVO}_4 \cdot 2.6\text{H}_2\text{O}$ and crystallized LiNiVO_4 (which adopts the spinel structure) can reversibly react with 7.5 and 6 Li ions per formula unit, respectively, leading to a practical capacity of about 1100 mA h/g (Fig. 3). Similarly as reported in Section 4.1, a smaller irreversible capacity loss is observed for the crystallized phase. This result can be linked with the BET surface area, which is larger for the amorphous hydrated vanadate. The larger the surface area, the larger

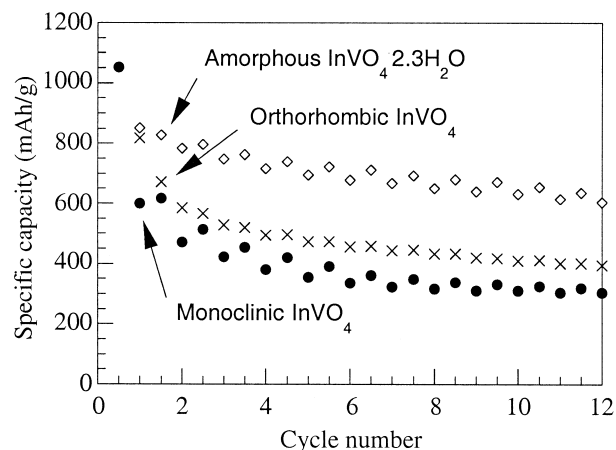


Fig. 5. Cycling behavior for InVO_4/Li Swagelok cells using either amorphous $\text{InVO}_4 \cdot 2.3\text{H}_2\text{O}$ or crystallized InVO_4 as the positive electrode.

Table 3

Comparison of the number of lithium ions which reversibly react with isostructural RVO_4 compounds

Compound	Δx_{rev}
Orthorhombic $InVO_4$	7
Orthorhombic $CrVO_4$	0
Monoclinic $InVO_4$	5
Monoclinic $CrVO_4$	2
Triclinic $FeVO_4$	7
Triclinic $AlVO_4$	0

the amount of adsorbed water, and therefore, the larger the amount of irreversible loss expected. Another feature for both amorphous and crystallized vanadates concerns the poor retention capacity upon cycling (Fig. 4).

4.3. RVO_4 ($R = In, Cr, Fe, Al$)

In the case of trivalent element-based vanadates, the synthesis leads to amorphous hydrated precursors, which produce crystallized phases depending on the annealing temperature.

An electrochemical investigation has confirmed the great interest of amorphous vanadates as the negative electrode material in Li-ion rechargeable batteries [2] (Fig. 5).

We also clearly showed that the electrochemical performances are strongly dependent on the nature of the trivalent element R. In Table 3 are listed the number of lithium ions reversibly introduced in crystallized RVO_4 ($R = In, Cr, Fe, Al$) compounds. These results prove that R is directly involved in the lithium reaction process. For instance, indium and iron vanadates display reversible capacities as large as 900 mA h/g while aluminum and chromium vanadates are not electroactive materials. Furthermore, lithium reaction in mixed $Cr_{0.5}In_{0.5}VO_4$ compounds (isostructural with orthorhombic $CrVO_4$ and $InVO_4$) emphasizes the great importance of the trivalent element, and more specifically, the inauspicious role of

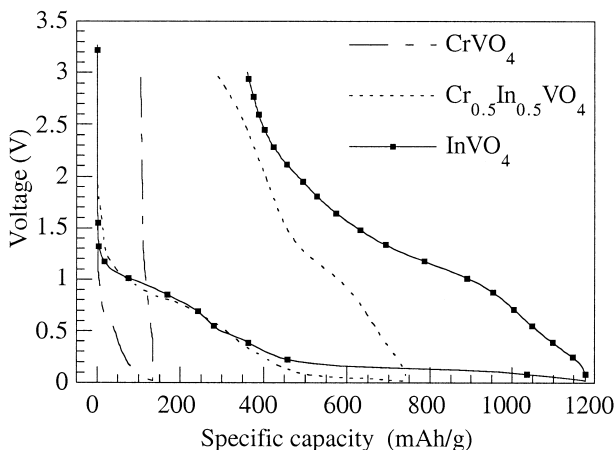


Fig. 6. Evolution of the voltage-composition profile curves for orthorhombic $Cr_x In_{1-x} VO_4$ vanadates ($x = 1, 0.5$ and 0).

chromium on the electrochemical performances of these vanadates (Fig. 6).

As an attempt to throw some light on the lithium reaction mechanism, in situ XRD and ex situ XANES measurements starting from crystallized $FeVO_4$ (triclinic symmetry) have been carried out [7].

4.4. In situ XRD study of crystallized $FeVO_4$

A cell using crystallized $FeVO_4$ as the cathode material was discharged to 0.02 V, and then charged to 3.5 V at a constant current rate of 0.03 mA. XRD patterns were collected approximately every 0.125 lithium reacted. Typi-

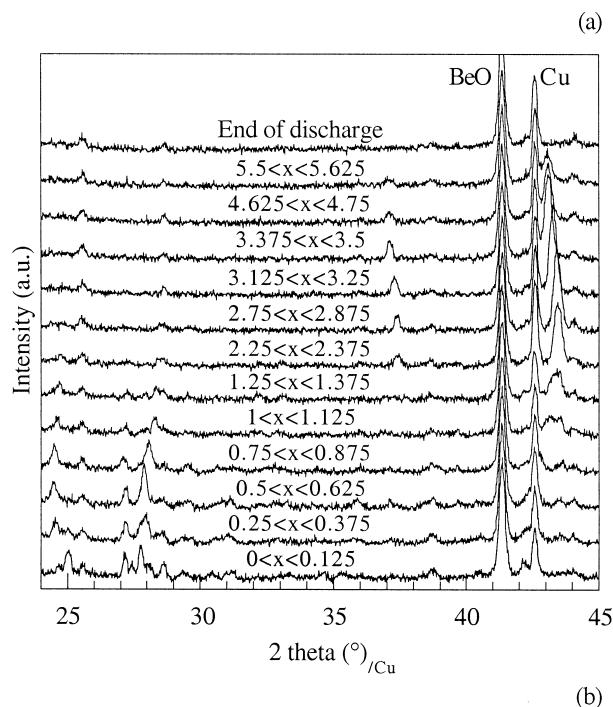


Fig. 7. In situ X-ray diffraction measurements for an electrochemical cell using triclinic $FeVO_4$ as the positive electrode material and Li as the negative electrode. (a) represents the most significant XRD patterns obtained during the in situ measurement; (b) shows the first cycle of such a battery.

cal scans ranged from 24–45° (2θ) in steps of 0.02° (2θ), and a fixed counting time (18 s) was employed.

Fig. 7a shows the most significant XRD patterns collected during the first electrochemical discharge of a FeVO_4/Li cell.

At $x = 0$, the XRD pattern is characteristic of triclinic FeVO_4 with, in addition, Bragg peaks corresponding to metallic copper (current collector) and beryllium oxide.

For $0.125 < x < 0.625$, new Bragg peaks (the main ones are located at 24.5, 27.2 and 28° (2θ)) appear, and grow in intensity while the intensity of the peaks corresponding to FeVO_4 decreases, and these reflections finally vanish. For $0.625 < x < 1.125$, a slight shift in the position of these Bragg reflections characteristic of a solid solution and a decrease in their intensity are noted, in agreement with the potential–composition curve (Fig. 7b) which indicates a smooth decay of the potential in this region.

For $x \sim 1.2$, the voltage dramatically drops from 2.1 V to 0.7 V. This corresponds to the formation of a new phase as shown in Fig. 7a. Indeed, beyond $x = 1$, new Bragg peaks located at 37.4 and 43.5° (2θ) appear and grow. This new phase becomes unique at $x = 2.5$, and was indexed in a cubic system with a lattice parameter $a = 4.16$ Å (S.G.: $Fm\bar{3}m$).

Upon further discharging the cell ($x > 2.5$), the Bragg peaks corresponding to this new cubic phase slightly shift in position, and decrease in intensity to completely vanish, resulting in a featureless XRD pattern characteristic of an amorphous material. During the following charges and discharges of the cell, the XRD patterns remain featureless.

4.5. XANES measurements

XANES data have been collected at the vanadium and iron K edges at some remarkable points, referenced from A to E in Fig. 7b, of the first electrochemical cycle curve.

The structure of the starting material FeVO_4 consists of a tridimensional packing of VO_4 tetrahedra, FeO_6 octahedra, and also FeO_5 trigonal bipyramids [8].

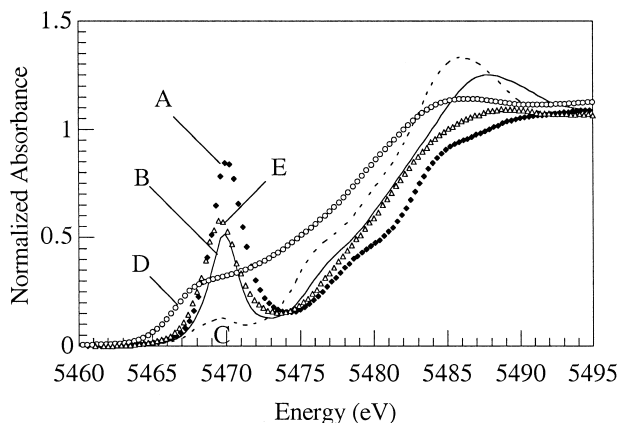


Fig. 8. Vanadium K edge for various lithium contents.

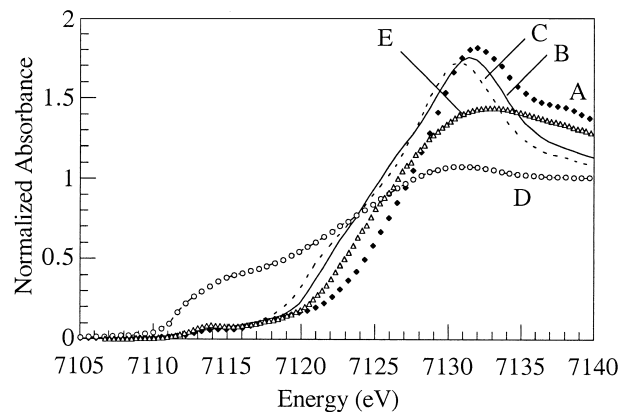


Fig. 9. Iron K edge for various lithium contents.

Dramatic modifications are induced during lithium reaction, as shown in Figs. 8 and 9. XANES data clearly indicate that vanadium atoms move from tetrahedra to square pyramids (sample B, $x = 1.3$) and then to slightly distorted octahedra (sample C, $x = 3.4$), with a large decrease in the prepeak intensity in the vanadium edge. The vanadium oxidation state has been reduced from 5 to about 3.5, with a shift in the edge position to lower energy. Concerning the oxygen environment of iron atoms, almost nothing has changed: they are located in a distorted octahedron, and the oxidation state is almost 2.5.

For sample D (end of the discharge), the profile curve is quite similar for both vanadium and iron K edges. Due to its flat form, no information can be given either on the oxidation state or on the local environment of vanadium and iron atoms. On the contrary, at the end of the charge (sample E), the vanadium goes back to a square pyramidal environment, and the iron remains in a distorted octahedron. Their oxidation states are almost 4 and 2.7, respectively.

5. Discussion

Our electrochemical results confirm that the vanadates are indeed of potential interest for application as negative electrode in lithium batteries. Indeed, it was shown that they can react with a large amount of lithium at a low mean voltage.

From in situ XRD measurements, we have seen that during the first discharge, several new phases appeared followed by the amorphization of the electrode. On the other hand, XANES data collected during the first electrochemical discharge of a FeVO_4/Li battery demonstrated that neither Fe nor V were completely reduced to the metallic state. Therefore, the reaction of eight lithium ions with this material cannot be explained through this method. However, these results strongly suggest that a Li uptake/removal mechanism different from the usual Li insertion/deinsertion process should happen. It was recently proposed [2] that (1) a decomposition process oc-

curred during the first discharge leading to a mixture of an inert matrix Li–M–O and of an electrochemically active Li–V–O phase and (2) the oxygen was acting as a redox center leading to possible ‘Li–O’ bonds thereby leading to the enhanced observed capacity.

This scenario was also proposed by Leroux et al. [9] concerning lithium introduction in molybdenum oxides, namely $\text{Na}_{0.25}\text{MoO}_3$. Thanks to ^7Li NMR and XAS experiments, these authors demonstrated the occurrence of a decomposition mechanism (leading to a ‘Li–O’ matrix together with a lithium molybdenum suboxide). They also pointed out the necessity of oxygen transport during the discharge/charge process. On the other hand, we can quote the work of Ceder et al. [10] on LiMO_2 ($M = \text{Ti, V, Mn, Co, Ni, Zn}$). By means of a series of computational experiments, they found that Li intercalation causes significant electron transfer to the oxygen ions in the structure. All these results demonstrate that the oxygen anion role is no longer transparent to the mechanism of insertion/deinsertion in such compounds.

However, experiments performed on vanadates cannot allow us to precisely determine the mechanism, and only some response elements have been proposed. More experiments are in progress in order to determine it.

6. Conclusion

A ‘chimie douce’ method, in which pH is a key parameter, has been successfully applied to the synthesis of several classes of vanadates, either amorphous or crystallized depending on both the nature of the counter cation and the isopolyanion species. Referring to the charge–pH diagram described by Livage et al. [6], we can roughly

predict the pH range within which a wished compound can be obtained.

An electrochemical investigation has shown that vanadates can react with large amounts of lithium at a low mean voltage so that some of these phases can be of potential interest as negative electrode materials in rechargeable Li-ion batteries. However, some problems in particular remain on the cycling efficiency. It is a must to overcome this capacity fading in order to implement these materials in practical Li-ion batteries.

In situ XRD and ex situ XANES measurements allowed us to give some elements in the understanding of the Li uptake/removal mechanism but further work is needed in order to propose a definitive mechanism.

References

- [1] C. Sigala, D. Guyomard, Y. Piffard, M. Tournoux, C.R. Acad. Sci. Paris, t. 320, Série IIB (1995), 523.
- [2] S. Denis, E. Baudrin, M. Touboul, J.-M. Tarascon, J. Electrochem. Soc. 144 (12) (1997) 4099.
- [3] E. Baudrin, S. Denis, F. Orsini, L. Seguin, M. Touboul, J.-M. Tarascon, J. Mat. Chem. 9 (1999) 101.
- [4] F. Orsini, E. Baudrin, S. Denis, L. Dupont, M. Touboul, D. Guyomard, Y. Piffard, J.-M. Tarascon, Solid State Ionics 107 (1998) 123.
- [5] M.T. Pope, in: Heteropoly and isopoly oxometalates, Springer Verlag, 35 (1983).
- [6] J. Livage, M. Henry, C. Sanchez, Prog. Solid State Chem. 38 (1988) 259.
- [7] S. Denis, Thesis, Amiens, France, 1998.
- [8] B. Robertson, E. Kostiner, J. Solid State Chem. 4 (1972) 29.
- [9] F. Leroux, G.R. Gowards, W.P. Power, L.F. Nazar, Electrochem. Solid State Lett. 1 (1998) 255.
- [10] G. Ceder, M.K. Aydinol, A.F. Kohan, Computational Materials Science, 394 (1997), in press.